Paper: Rb24-4-5505

Bio-Inspired Feedback Control of Three-Dimensional Humanlike Bipedal Robots

Ryan W. Sinnet and Aaron D. Ames

Department of Mechanical Engineering, Texas A&M University
200 MEOB, 3123 TAMU, College Station, Texas 77843-3123, USA
E-mail: {rsinnet, aames}@tamu.edu
[Received 00/00/00; accepted 00/00/00]

Bridging contemporary techniques in bio-inspired control affords a unique perspective into human locomotion where the interplay between sagittal and coronal dynamics is understood and exploited to simplify control design. Functional Routhian reduction is particularly useful on bipeds as it decouples these dynamics, allowing for control design on a sagittally-restricted model while providing coronal stabilization. 2D sagittal walking is designed using Human-Inspired Control which produces humanlike walking with good stability properties. This walking is then easily translated to 3D via reduction. The proposed control scheme, which is based on a fundamental understanding of human walking, is validated in both simulation and experiment.

Keywords: bipedal robotic walking, geometric reduction

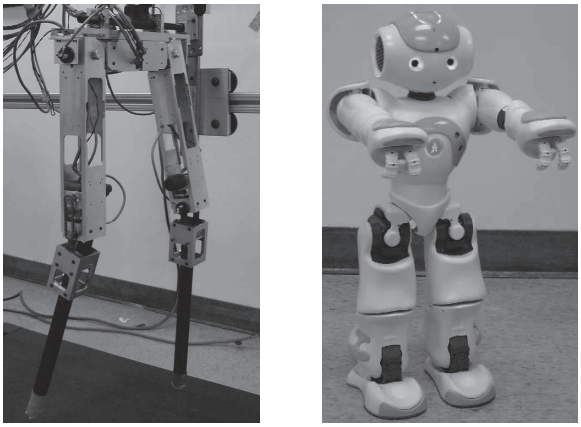

Fig. 1. The models of interest are based on the robots AMBER (left) and NAO (right).

1. Introduction

Robotic walking is often studied with little direct inspiration from human locomotion. If the goal is to achieve humanlike walking, then existing approaches have been largely unsuccessful: walking has been achieved using a variety of strategies – passivity-based control [1], zero moment point [2], hybrid zero dynamics [3], etc. – yet the gaits have been generally non-humanlike [4]. This paper weaves together existing methods, proposing a procedure to produce 3D walking by fusing Human-Inspired Control [5], hybrid zero dynamics [3], and functional Routhian reduction [6].

Many existing methods are effective, yet the control schemes are often esoteric and obfuscate the underlying mathematical foundation of human walking. Human-Inspired Control, on the other hand, asserts that there is elegance to be found in simplicity. Indeed, by examining human kinematics data, it becomes apparent that certain kinematics outputs of human walking, termed *human outputs*, can be encoded with very little loss by fitting the data to *canonical walking functions*, which have the same form as the solution to a linear spring-mass-damper system. In addition, the methods of hybrid zero dynamics are drawn upon to construct a *zero dynamics* which can be rendered forward-invariant through feedback linearization, and is, moreover, invariant through impacts (i.e., foot strike), resulting in guaranteed stability properties [7, 8].

After achieving 2D walking, *functional Routhian reduction* is used to migrate the controller to a 3D model. In order to combine this with Human-Inspired Control, it is necessary to extend previous results [9] as was done in [6] to include systems with forcing. In this paper, a formal proof is given for the theorem stated in [6]. The appeal of functional Routhian reduction comes from its capacity to separate sagittal and coronal dynamics, permitting control design for each to be conducted independently and exposing the decoupled nature of human walking. Stable 3D walking for models based on AMBER and NAO (shown in **Fig. 1**) is achieved using a sagittal control law designed on a reduced-order model. Simulation results show that the 2D and 3D gaits for each robot are virtually identical. An experiment with NAO validated the control scheme by showing relatively robust and humanlike walking.

The rest of this paper is structured as follows: Section 2 introduces a general formulation for the robotic models of interest. Section 3 reviews Human-Inspired Control and applies it to achieve 2D walking in simulation. Section 4 details functional Routhian reduction and Section 5 uses this reduction to migrate the 2D walking to 3D. Section 6 discusses simulation of the 3D models and concludes by providing analysis of a walking experiment conducted with NAO.

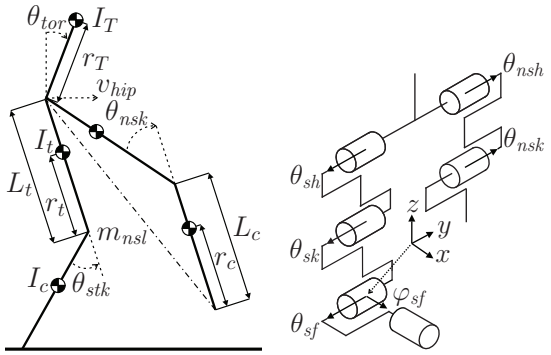

Fig. 2. General model of interest showing configuration variables (right) and physical and human outputs (left).

2. Robotic Modeling

Bipedal walking exhibits both continuous dynamics – when the non-stance leg swings freely – and discrete dynamics, consisting of periodic impacts when the non-stance foot strikes the ground. The necessity to model both types of dynamics, which operate on very different time scales, motivates the use of *hybrid systems* or *systems with impulse effects* [10]. In order to establish the stability of hybrid periodic orbits, the standard technique of studying the Poincaré map [11] is used. Although it is not possible to explicitly compute the Poincaré map for most bipeds, one can compute a numerical approximation through simulation and thereby ascertain stability. The two robots studied, AMBER[1] and NAO[2], will be modeled as in **Fig. 2** using a hybrid control system,

$$\mathscr{HC}_{3\mathrm{D}} = (D, U, S, \Delta, f, g), \quad (1)$$

which is standard in the literature [12]. Denote the mechanical configuration Q with coordinates

$$q = (\varphi_{sf}, \theta_{sf}, \theta_{sk}, \theta_{sh}, \theta_{nsh}, \theta_{nsk})^T. \quad (2)$$

The *domain* $D \subset TQ$ represents the admissible configurations, $U \subseteq \mathbb{R}^6$ is the set of *admissible controls*, $S \subset D$ is a *guard* or *switching surface* which represents the edge of the domain, $\Delta : S \to D$ is a smooth map called the *reset map*, and (f,g) is a *control system* on D.

The Lagrangian, $L : TQ \to \mathbb{R}$, can be stated in terms of kinetic energy, $K : TQ \to \mathbb{R}$, and potential energy, $V : Q \to \mathbb{R}$, as $L(q,\dot{q}) = T(q,\dot{q}) - V(q)$. The forced Euler-Lagrange equation gives the dynamic model, which, for robotic systems (see [13]), takes the form: $M(q)\ddot{q} + H(q,\dot{q}) = \Upsilon$, with inertia map $M : Q \to \mathbb{R}^{n\times n}$ and forcing Υ and $H(q,\dot{q}) = C(q,\dot{q})\dot{q} + N(q)$ containing terms resulting from the Coriolis effect and gravity. This corresponds to the vector field

$$f(q,\dot{q}) = \begin{bmatrix} \dot{q} \\ M^{-1}(q)\left(\Upsilon - H(q,\dot{q})\right). \end{bmatrix} \quad (3)$$

In this paper, forcing takes the form $\Upsilon = B(q)u$ with torque distribution map $B : Q \to \mathbb{R}^{n\times n}$. This results in the control system (f,g):

$$f(q,\dot{q}) = \begin{bmatrix} \dot{q} \\ -M^{-1}(q)H(q,\dot{q}) \end{bmatrix},\ g(q) = \begin{bmatrix} \mathbf{0}_{n\times n} \\ M^{-1}(q)B(q) \end{bmatrix} \quad (4)$$

The impact model in [14] is used which considers rigid-body, plastic impacts. Impulsive forces are applied to the non-stance foot when it contacts the ground. This results in an *impact map* which gives post-impact velocities [5]. And, finally, a reduced-order model for the purpose of sagittal controller design is obtained by applying a *sagittal restriction* to the full-order model:

$$\mathscr{HC}_{2\mathrm{D}} = (D_{2\mathrm{D}}, U_{2\mathrm{D}}, S_{2\mathrm{D}}, \Delta_{2\mathrm{D}}, f_{2\mathrm{D}}, g_{2\mathrm{D}}). \quad (5)$$

This is as simple as setting $\varphi = 0$ and projecting away this coordinate from the hybrid model $\mathscr{HC}_{3\mathrm{D}}$.

3. Human-Inspired Control

The framework of Human-Inspired Control was recently developed as a method of achieving humanlike walking on robots [7, 8, 12]. Its appeal lies in the simple structure of the fundamental underlying mathematical element: the *canonical walking function*. This function can faithfully represent the human gait when fit to specific kinematics outputs. When applied via control to a biped, the canonical walking function yields qualitatively and quantitatively humanlike locomotion. Moreover, a partial hybrid zero dynamics is generally constructed [7] by imposing constraints during the fitting process, i.e., constrained optimization, resulting in guaranteed stability.

Gait Analysis. Kinematics outputs on the data in [4] were averaged between subjects and then analyzed. These *human outputs* can be computed as forward kinematics maps on a robot. Natural course of thought, then, leads one to suppose that if the robot outputs match the human outputs, the gait ought to be humanlike. This bridge between human walking and humanlike robots is the conceptual foundation beneath Human-Inspired Control.

The Canonical Walking Function. Analysis of kinematics outputs yielded five choices which, together, appear to faithfully represent human walking (see **Fig. 3**):

O1 : p_{hip}, the x-position of the hip;

O2 : m_{nsl}, the slope of the non-stance leg;

O3 : θ_{sk}, the angle of the stance knee from straight;

O4 : θ_{nsk}, the angle of the non-stance knee from straight; and

O5 : θ_{tor}, the angle between the torso and vertical.

It was discovered in [7, 12] that the human outputs **O2**–**O5** can be accurately described by a *single* function – the time solution to a linear spring-mass-damper system – termed the *canonical walking function*:

$$y_i^H(t,\alpha) = e^{-\alpha_{i,4}t}\left(\alpha_{i,1}\cos(\alpha_{i,2}t) + \alpha_{i,3}\sin(\alpha_{i,2}t)\right) + \alpha_{i,5}, \quad (6)$$

1. http://www.bipedalrobotics.com/
2. http://www.aldebaran-robotics.com/

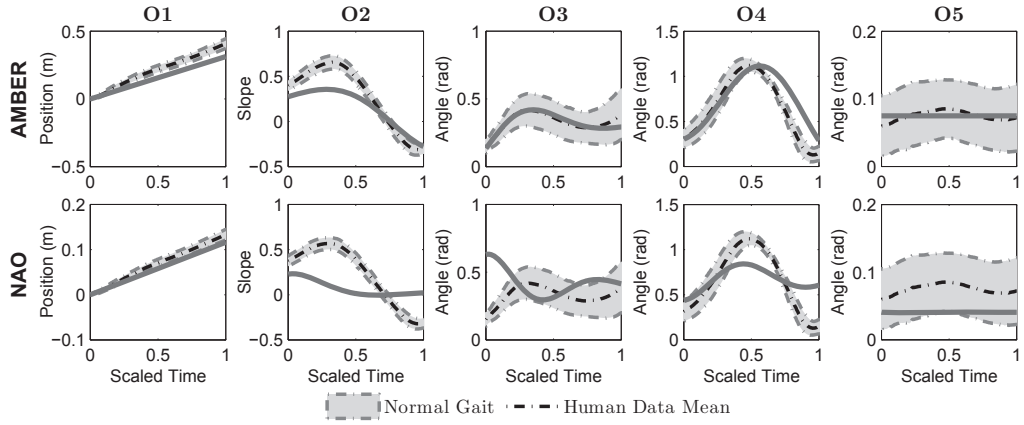

Fig. 3. Optimized human functions for AMBER and NAO compared with normal human walking. The humanlike nature of the encoded walking can be seen with respect to each human output.

where $i \in \{2,\dots,5\}$ is an index corresponding to outputs **O2–O5**. The parameters are combined into a matrix:

$$\alpha = \begin{pmatrix} v_{hip} & \mathbf{0}_{1\times 4} \\ \{\alpha_i\}_{i\in\{2,\dots,5\}} & \end{pmatrix} \in \mathbb{R}^{5\times 5}$$

Observe that Eq. (6) is the solution of a linear spring-mass-damper system for which $\alpha_{i,1}$ and $\alpha_{i,3}$ would be determined from initial conditions, $\alpha_{i,4} = \zeta\omega_n$ with damping ratio ζ and undamped natural frequency ω_n, $\alpha_{i,2} = \omega_d$ with damped natural frequency ω_d, and $\alpha_{i,5}$ is the gravity bias. It was shown in [7] that these functions can be fit to human outputs with correlation coefficients near unity.

Time-Invariant Parameterization. In order to achieve *autonomous* control, time is replaced by a state-based parameterization as is common in the literature [3]. Denote this parameterization $\tau : Q_{2\mathrm{D}} \to \mathbb{R}_0^+$ where $\mathbb{R}_0^+$ represents time. From **Fig. 3**, it is clear that the position of the hip, $p_{hip}(q)$, increases monotonically during the gait and is thus a good choice for τ. Thus, define

$$\tau(\theta) := \frac{p_{hip}(\theta) - p_{hip}(\theta^-)}{v_{hip}}, \quad \dots\dots\dots \quad (7)$$

where v_{hip} represents the desired hip velocity and $p_{hip}(\theta^-)$ is the hip position at the beginning of a step.

Sagittal Controller Construction. This paper achieves 3D walking by using reduction to decouple the sagittal and coronal dynamics of $\mathscr{HC}_{3\mathrm{D}}$, thereby enabling independent control design. The construction of the sagittal controller consists of 1) finding parameters of the canonical walking function (Eq. (6)) such that a *hybrid zero dynamics* is created and 2) using these parameters with the output functions to construct a sagittal walking controller.

Hybrid Zero Dynamics. The goal of the controller is to drive the outputs of the robot to the canonical walking functions. Therefore, define the actual outputs

$$y_a(\theta) = (p_{hip}(\theta), m_{nsl}(\theta), \theta_{stk}, \theta_{swk}, \theta_{tor}(\theta))^T,$$

which combines the outputs **O1–O5** computed for the robot from its kinematics, and the controller outputs, $y : Q_{2\mathrm{D}} \to \mathbb{R}^5$, and their derivatives, $\dot{y} : TQ_{2\mathrm{D}} \to \mathbb{R}^5$, as

$$y_i(\theta) = \begin{cases} 0, & i = 1, \\ y_i^a(\theta) - y_i^H(\tau(\theta), \alpha_i), & i = 2,\dots,5, \end{cases}$$
$$\dot{y}_i(\theta,\dot{\theta}) = \begin{cases} \dot{p}_{hip}(\theta,\dot{\theta}) - v_{hip}, & i = 1, \\ \dfrac{d}{dt} y_i(\theta,\dot{\theta}), & i = 2,\dots,5. \end{cases}$$
$$\dots\dots\dots\dots\dots \quad (8)$$

where $y_i^H(\theta)$ are the canonical walking functions of Eq. (6) with time parameterized by Eq. (7). For these outputs, the *zero dynamics* $\mathbf{Z}_\alpha$ is the surface on which the actual and desired outputs agree for all time, i.e., $y(\theta) \equiv \dot{y}(\theta,\dot{\theta}) \equiv 0$. Due to the nature of impacts, it is unlikely the hip velocity will remain constant through impact; thus the *partial zero dynamics* $\mathbf{PZ}_\alpha$ is also an important construct – this is the surface where $y_i(\theta) \equiv \dot{y}_i(\theta,\dot{\theta}) \equiv 0$, $i \in \{2,\dots,5\}$. See [7] for a more formal definition of these surfaces.

The main result of [7] is that, using the controller outputs of Eq. (8) with feedback linearization, it is possible to realize a parameter matrix α which produces stable walking. This is stated in the form of an optimization problem. From the mean human walking data, denote by $\tau^{\mathrm{HD}}[k]$ and $y_i^{\mathrm{HD}}[k]$ the sampled times and values, respectively, of the output functions **O1–O5**. Then define the cost

$$\mathrm{Cost}_{\mathrm{HD}}(\alpha) = \sum_{k=1}^{K}\sum_{i=1}^{5} \left(y_i^{\mathrm{HD}}[k] - y_i^H(\tau^{\mathrm{HD}}[k],\alpha)\right)^2. \quad (9)$$

Minimizing this subject to constraints which ensure stable robotic walking results in a least-squares fit of the canonical walking functions to the mean human data, thus motivating the optimization problem.

$$\alpha^* = \underset{\alpha\in\mathbb{R}^{5\times 5}}{\operatorname{argmin}} \ \mathrm{Cost}_{\mathrm{HD}}(\alpha) \quad \dots\dots\dots \quad (10)$$
$$\text{s.t.} \qquad \Delta_{2\mathrm{D}}(S_{2\mathrm{D}} \cap \mathbf{Z}_\alpha) \in \mathbf{PZ}_\alpha$$

Solving numerically in MATLAB through `fmincon` results in a matrix of parameters for both AMBER and NAO. In [7], it was shown that conditions on Eq. (10) can be given in terms of *only* α. The proximity of the optimized gaits to normal human walking is shown in **Fig. 3**.

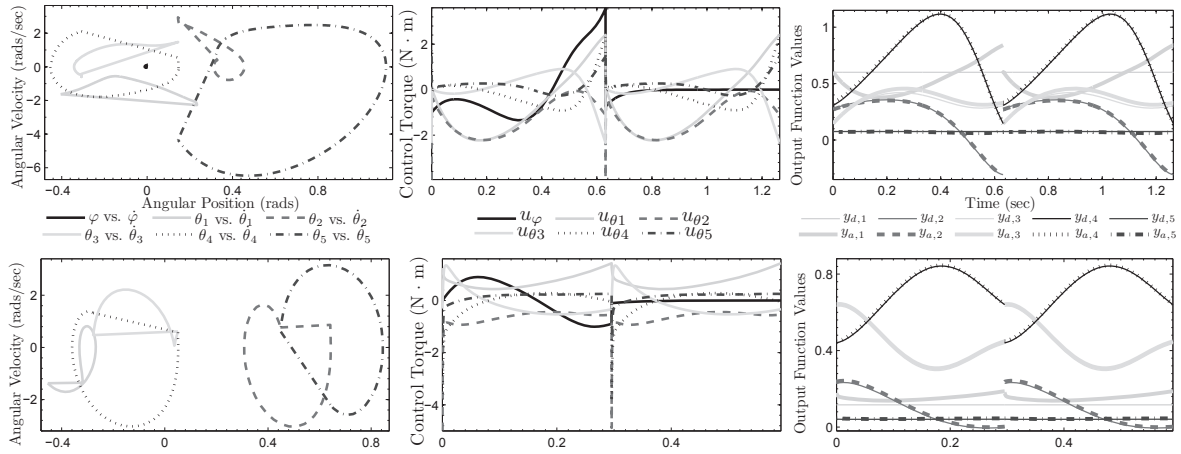

Fig. 4. Simulation of three-dimensional biped models for AMBER (top) and NAO (bottom). Phase portraits are shown (left) along with input torques (middle) and output function values (right).

Controller Design. The optimization begets stable walking when paired with feedback linearization, yet the desire to employ functional Routhian reduction precludes the application of such a control law in sagittal design as it is not independent of the coronal variables. This will be seen later in Theorem 1. Proportional-Derivative (PD) control, on the other hand, does not suffer the same limitation and is thus used instead. Define the control law

$$K^{\alpha}_{2\mathrm{D}}(\theta,\dot{\theta}) = -k_p\, y(\theta) - k_d\, \dot{y}(\theta,\dot{\theta}) \quad . \quad . \quad . \quad . \quad . \quad (11)$$

This is applied to the system $\mathscr{HC}_{2\mathrm{D}}$ to obtain $\mathscr{H}^{\alpha}_{2\mathrm{D}}$.

Simulation. Simulations for AMBER and NAO were conducted choosing $k_p = 50$ and $k_d = 20$. The 2D phase portraits are nearly identical to the 3D ones in **Fig. 4** and are, therefore, omitted; there exists a closed limit cycle for each model representing steady-state walking. The humanlike nature of the gaits can be ascertained from the fits in **Fig. 3**. The gait of AMBER is more humanlike than that of NAO, presumably as a consequence of AMBER having proportions more similar to a human than does NAO.

Stability is confirmed by locating a fixed point and examining the Poincaré maps linearized about those points. The maximum eigenvalues of AMBER (resp. NAO) are found to have magnitudes 0.409 (resp. 0.700).

4. Functional Routhian Reduction

Classical Routhian reduction [15] is a method which takes advantages of symmetries inherent in a dynamical system and utilizes conserved momentum to eliminate cyclic variables, thereby reducing the dimensionality of the system and simplifying controller design. *Functional Routhian reduction* (first introduced in [16, 17]) is a variant in which the conserved momentum is set to a function rather than a constant. This scheme has enjoyed success in migrating 2D gaits to 3D [6, 9]. By decoupling the sagittal and coronal dynamics, functional Routhian reduction provides insight into the decoupled nature of human walking and allows for sagittal control design to be conducted on a reduced-order model while simultaneously providing coronal stabilization. This remarkable relationship between dynamics, while only providing a slight reduction in dimensionality, shifts the control problem from designing complicated 3D walking gaits to the much more tractable challenge of designing 2D gaits. Thus, stable walking is obtained in 3D by simply applying control laws which give stable walking in the sagittally-restricted counterpart in 2D (which has a Lagrangian of the form given in Eq. (15)).

Almost-Cyclic Lagrangians. Consider a system with configuration space $Q = \mathbb{S} \times S$, where S is called the *shape space*. Let the coordinates be represented by $q = (\varphi, \theta^T)^T$ with $\theta \in S$ and *almost-cyclic* variable $\varphi \in \mathbb{S}$. A Lagrangian $L_\lambda : T\mathbb{S} \times TS \to \mathbb{R}$ is almost-cyclic if it takes the form in Eqs. (10) and (11) from [6] for some $\lambda : \mathbb{S} \to \mathbb{R}$.

Momentum Maps. As alluded to earlier, functional Routhian reduction utilizes a momentum map, $J : TQ \to \mathbb{R}$, which specifies conserved quantities:

$$J(\varphi,\theta,\dot{\varphi},\dot{\theta}) = \frac{\partial L_\lambda}{\partial \dot{\varphi}} = M_{\varphi,\theta}(\theta)\,\dot{\theta} + m_\varphi(\theta)\,\dot{\varphi}. \quad (12)$$

This map is equal to a function, $\lambda(\varphi)$.

Functional Routhians. For an almost-cyclic Lagrangian L_λ, define the *functional Routhian* $L_{\mathrm{fct}} : TS \to \mathbb{R}$:

$$L_{\mathrm{fct}}(\theta,\dot{\theta}) = \left[L_\lambda(\varphi,\theta,\dot{\varphi},\dot{\theta}) - \lambda(\varphi)\,\dot{\varphi}\right]_{J(\varphi,\theta,\dot{\varphi},\dot{\theta})=\lambda(\varphi)}. \quad (13)$$

Because $J(\varphi,\theta,\dot{\varphi},\dot{\theta}) = \lambda(\varphi)$ implies that

$$\dot{\varphi} = \frac{1}{m_\varphi(\theta)}(\lambda(\varphi) - M_{\varphi,\theta}(\theta)\,\dot{\theta}) \quad . \quad . \quad . \quad . \quad . \quad (14)$$

by direct calculation the functional Routhian is given by:

$$L_{\mathrm{fct}}(\theta,\dot{\theta}) = \frac{1}{2}\dot{\theta}^T M_\theta(\theta)\,\dot{\theta} - V_{\mathrm{fct}}(\theta). \quad . \quad . \quad . \quad (15)$$

Reduction Theorem. Before introducing the reduction theorem, note that for L_λ with forcing $\Upsilon(q,\dot{q})$, the Euler-

Lagrange equation can be written:

$$\frac{d}{dt}\frac{\partial L_\lambda}{\partial \dot{q}} - \frac{\partial L_\lambda}{\partial q} = M_\lambda(\theta)\ddot{q} + H_\lambda(\theta,\dot{\theta}) + y_\lambda(\varphi,\theta,\dot{\theta}) - \Upsilon(q,\dot{q}), \quad . \quad (16)$$

where $H_\lambda(\theta,\dot{\theta})$ is obtained from $M_\lambda(\theta)$ and

$$y_\lambda(\varphi,\theta,\dot{\theta}) = \frac{d}{dt}\frac{\partial W_\lambda}{\partial \dot{q}} - \frac{\partial W_\lambda}{\partial q}.$$

This can be written as the vector field

$$f_{L_\lambda}(q,\dot{q}) = \begin{pmatrix} \dot{q} \\ M_\lambda^{-1}(\theta)(\Upsilon(q,\dot{q}) - H_\lambda(q,\dot{q}) - y_\lambda(\varphi,\theta,\dot{\theta})) \end{pmatrix}. \quad (17)$$

In addition, $f_{L_{\text{fct}}}$, the forced vector field corresponding to L_{fct}, is given by Eq. (3). The solutions of these two systems are related in the following manner (in a way analogous to the classical Routhian reduction result, see [15]).

Theorem 1: *Let L_λ be an almost-cyclic Lagrangian with almost-cyclic variable φ and L_{fct} its functional Routhian with shape space $S = \mathbb{R}^{n-1}$. Additionally, let $\Upsilon : TQ \to \mathbb{R}^n$ represent external forcing satisfying*

(i) $\Upsilon(q,\dot{q}) = \Upsilon(\theta,\dot{\theta})$, *i.e., Υ does not depend on $\varphi, \dot{\varphi}$,*

(ii) $\Upsilon_\varphi(\theta,\dot{\theta}) = 0$, *i.e., no external forces act on the almost-cyclic variable.*

Then, $(\varphi(t),\theta(t),\dot{\varphi}(t),\dot{\theta}(t))$ is a solution to the vector field f_{L_λ} given by Eq. (17) on $[t_0,t_F]$ with

$$\dot{\varphi}(t_0) = \frac{1}{m_\varphi(\theta(t_0))}(\lambda(\varphi(t_0)) - M_{\varphi,\theta}(\theta(t_0))\,\dot{\theta}(t_0)) \quad (18)$$

if and only if $(\theta(t),\dot{\theta}(t))$ is a solution to $f_{L_{\text{fct}}}$ given by Eq. (3) and $(\varphi(t),\dot{\varphi}(t))$ satisfies:

$$\dot{\varphi}(t) = m_\varphi^{-1}(\theta(t))(\lambda(\varphi(t)) - M_{\varphi,\theta}(\theta(t))\,\dot{\theta}(t)). \quad (19)$$

To prove this, first note that the Lagrangian can be written

$$L_\lambda(\varphi,\theta,\dot{\varphi},\dot{\theta}) = L_{\text{fct}}(\theta,\dot{\theta}) + \text{Rem}(\varphi,\theta,\dot{\varphi},\dot{\theta}),$$

where

$$\text{Rem}(\varphi,\theta,\dot{\varphi},\dot{\theta}) = \frac{m_\varphi(\theta)}{2}\dot{\varphi}^2 + \frac{1}{2}\frac{\lambda^2(\varphi)}{m_\varphi(\theta)} + \dot{\varphi}M_{\varphi,\theta}(\theta)\dot{\theta} + \frac{1}{2}\frac{1}{m_\varphi(\theta)}\dot{\theta}^T M_{\varphi,\theta}^T(\theta)M_{\varphi,\theta}(\theta)\dot{\theta} - \frac{\lambda(\varphi)}{m_\varphi(\theta)}M_{\varphi,\theta}(\theta)\dot{\theta}.$$

Application of the Euler-Lagrange equation gives

$$\frac{d}{dt}\frac{\partial L_\lambda}{\partial \theta_i} - \frac{\partial L_\lambda}{\partial \theta_i} = \frac{d}{dt}\frac{\partial L_{\text{fct}}}{\partial \dot{\theta}_i} - \frac{\partial L_{\text{fct}}}{\partial \theta_i} + \frac{d}{dt}\frac{\partial \text{Rem}}{\partial \dot{\theta}_i} - \frac{\partial \text{Rem}}{\partial \theta_i} = \Upsilon_i(\theta,\dot{\theta}),$$
$$\frac{d}{dt}\frac{\partial L_\lambda}{\partial \dot{\varphi}} - \frac{\partial L_\lambda}{\partial \varphi} = \frac{d}{dt}\frac{\partial \text{Rem}}{\partial \dot{\varphi}} - \frac{\partial \text{Rem}}{\partial \varphi} = 0, \quad . \quad . \quad (20)$$

where $i = 1,\ldots,\dim(S)$. It can be verified through direct calculation that the above are satisfied when the functional conserved quantity of Eq. (14) is satisfied.

Proof: ($\Rightarrow$) Let $(\varphi(t),\theta(t),\dot{\varphi}(t),\dot{\theta}(t))$ be a flow of f_{L_λ} given by Eq. (17) on $[t_0,t_F]$ with $\dot{\varphi}(t_0)$ satisfying Eq. (18) and let $(\vartheta(t),\dot{\vartheta}(t))$ be a flow of $f_{L_{\text{fct}}}$ given by Eq. (4) on $[t_0,t_F]$ with $\vartheta(t_0) = \theta(t_0)$ and $\dot{\vartheta}(t_0) = \dot{\theta}(t_0)$, and let $\phi(t)$ satisfy

$$\phi(t_0) = \varphi(t_0),$$
$$\dot{\phi}(t_0) = m_\varphi^{-1}(\phi(t))\left(\lambda(\phi(t)) - M_{\varphi,\theta}(\vartheta(t))\dot{\vartheta}(t)\right).$$

It follows from Eq. (20) that the curve $(\phi(t),\vartheta(t),\dot{\phi}(t),\dot{\vartheta}(t))$ satisfies the forced Euler-Lagrange equations corresponding to L_λ and is thus a flow of f_{L_λ} on $[t_0,t_F]$. Moreover, because both curves have the same initial conditions, it follows by uniqueness of solutions that

$$(\varphi(t),\theta(t),\dot{\varphi}(t),\dot{\theta})) = (\phi(t),\vartheta(t),\dot{\phi}(t),\dot{\vartheta}(t))$$

and therefore $(\theta(t),\dot{\theta}(t))$ is a flow of the vector field $f_{L_{\text{fct}}}$ on $[t_0,t_F]$ and $\dot{\varphi}(t)$ satisfies Eq. (19).

($\Leftarrow$) Let $(\theta(t),\dot{\theta}(t))$ be a flow of $f_{L_{\text{fct}}}$ on $[t_0,t_F]$ and $(\varphi(t),\dot{\varphi}(t))$ be a pair satisfying Eq. (19). It then follows from Eq. (20) that the forced Euler-Lagrange equations for L_λ are satisfied since the curve $(\theta(t),\dot{\theta}(t))$ satisfies the forced Euler-Lagrange equations for L_{fct} by definition and, therefore, $(\varphi(t),\theta(t),\dot{\varphi}(t),\dot{\theta}(t))$ is a solution to f_{L_λ} on $[t_0,t_F]$ satisfying Eq. (18). ■

5. Reduction Control Laws

Three controllers will be needed to obtain walking in the 3D model. The Human-Inspired Control introduced previously will provide sagittal control. In this section, two additional controllers are described. The first shapes the Lagrangian into an almost-cyclic Lagrangian which is amenable to reduction. In order to enjoy the decoupling effects of reduction, a second controller is needed to stabilize to the surface where reduction is valid.

Sagittal Control. The first controller is strictly responsible for motion in the sagittal plane. This controller will be used with the reduction controllers to generate walking for the three-dimensional model. In Section 3, a controller was described which resulted in walking for the sagittally-restricted model $\mathscr{HC}_{2\text{D}}$ given in Eq. (5). This exact control law, $K_{2\text{D}}^\alpha$, given by Eq. (11), is applied to the sagittal coordinates of the the 3D model $\mathscr{HC}_{3\text{D}}$.

Lagrangian Shaping Controller. Reduction is only valid for almost-cyclic Lagrangians motivating the use of control to shape the Lagrangian of the system into this form. Using $\lambda(\varphi) = -\mu\varphi$ with control gain $\mu \in \mathbb{R}^+$, the system can be shaped to be almost-cyclic with the control law

$$K_{3\text{D}}^{\alpha,\mu}(q,\dot{q}) = B_{3\text{D}}^{-1}(H_{3\text{D}}(q,\dot{q}) + M_{3\text{D}}(q)M_\mu^{-1}(\theta)[-H_\mu(q,\dot{q}) - y_\mu(\varphi,\theta,\dot{\theta}) + K_{3\text{D}}^\alpha(\theta,\dot{\theta})]) \quad . \quad . \quad . \quad . \quad . \quad . \quad . \quad . \quad . \quad . \quad . \quad (21)$$

where 3D and μ represent the nominal shaped system.

For initial conditions satisfying Eq. (18), the continuous dynamics of $\mathscr{HC}_{3\text{D}}$ can be decoupled into the sagit-

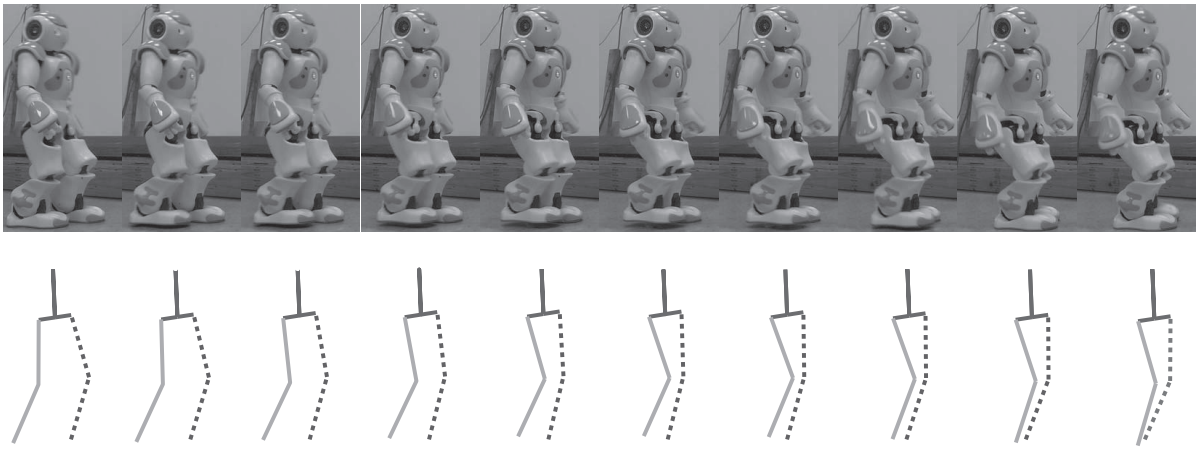

Fig. 5. Comparison of experimental and simulated walking gaits. The stance leg is represented by a dashed line and the nonstance leg is represented by a solid line. About half of the torso has been hidden due to space constraints.

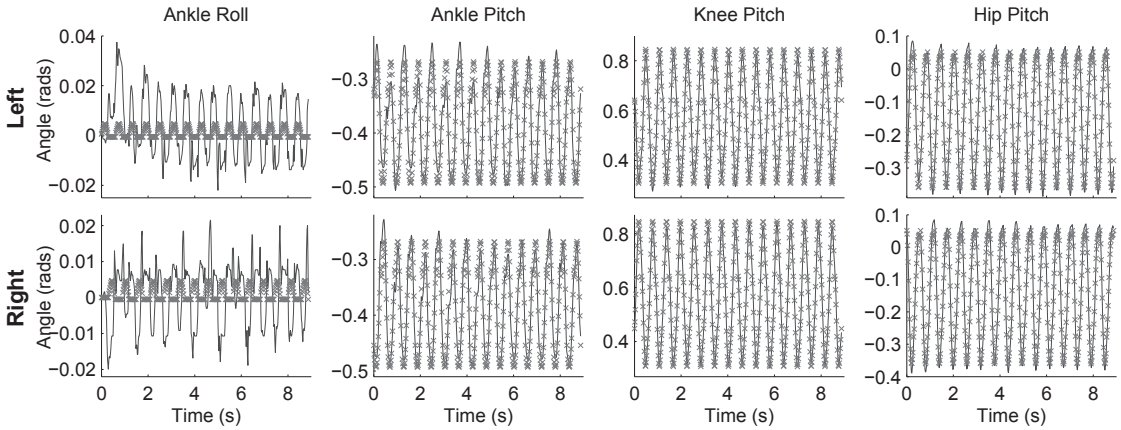

Fig. 6. Comparison between experiment and simulation for NAO. Left leg (top) and right leg (bottom). Black solid lines represent experimental data; gray dashed lines represent desired trajectories.

tal and coronal components with $K_{3D}^{\alpha,\mu}(q,\dot{q})$. This control law, in Eq. (21), contains the sagittal control law $K_{2D}(\theta,\dot{\theta})$. Furthermore, the dynamics of φ evolve according to Eq. (19). To guarantee the requirements of Eq. (19) are satisfied, an additional control law is needed. The assumptions of Theorem 1 are satisfied only on the zero dynamics

$$Z = \left\{ (q^T, \dot{q}^T)^T \in Q_{3D} : y_z(q,\dot{q}) = 0 \right\}, \quad \ldots \quad (22)$$

where

$$y_z(q,\dot{q}) = \dot{\varphi} + m_{\varphi}^{-1}(\theta)\left(\mu\varphi + M_{\varphi,\theta}(\theta)\,\dot{\theta}\right). \quad (23)$$

Feedback linearization allows this to be realized.

6. 3D Simulation and Experiment

Simulations were run choosing $\varepsilon = 20$ and $\mu = 1$. This resulted in stable walking which is strikingly similar to 2D simulations. The gait tiles in **Fig. 5** and phase portraits in **Fig. 4** show the humanlike nature of the gaits. The outputs and torques are shown in **Fig. 4** and are reasonable for the robots studied. A linearization of the Poincaré maps for AMBER (resp. NAO) results in maximum eigenvalues of magnitude 0.286 (resp. 0.300), indicating stable walking; and, moreover, the gaits have Specific Cost of Transport (SCOT) 0.35 (resp. 0.36), which are reasonably close to the human value of 0.20 [18]. The 2D and 3D walking gaits are virtually identical illustrating the decoupled nature of walking. This comparison highlights the utility of functional Routhian reduction, which seems to provide an intuitive way of implementing 2D walking gaits in 3D.

NAO Experiment. An experiment was conducted with NAO to substantiate the practicality of reduction-based, Human-Inspired Control. The experiment proved somewhat remarkable: on the first run, the robot achieved dynamically-stable walking with a forward velocity of 15 cm/s. The gait was implemented through trajectory tracking. The experiment was conducted on a laminate floor as shown in **Fig. 1**. The initial condition of the robot was chosen to be on the guard but with zero velocity and NAO was able to fall into the designed gait as shown in **Fig. 5**. This figure juxtaposes the simulated gait and NAO attempting to reproduce the simulated gait – one can see the agreement. Further evidence of agreement is provided by **Fig. 6**. The sagittal coordinates track closely while

the coronal coordinates have some error to them. This is likely the result of model differences and the relative magnitude of the coronal trajectories. Yet this walking is dynamically-stable, a feat which is difficult to achieve given the large size of NAO's feet. A video of the walking achieved in this experiment can be seen online[3] and the reader is invited to draw his or her own conclusions about the humanlike nature of the walking.

Acknowledgements

R. W. Sinnet is an NSF Graduate Research Fellow. This work is also supported by NSF grants CNS-0953823 and CNS-1136104 and NASA contract NNX12AB58G.

References:

[1] S. H. Collins, A. Ruina, R. Tedrake, and M. Wisse, "Efficient Bipedal Robots Based on Passive-Dynamic Walkers," Science, Vol.307, pp. 1082-1085, February 2005.

[2] M. Vukobratović and B. Borovac, "Zero-Moment Point – Thirty-Five Years of Its Life," Int. J. of Humanoid Robotics, Vol.1, No.1, pp. 157-173, March 2005.

[3] E. R. Westervelt, J. W. Grizzle, C. Chevallereau, J. H. Choi, and B. Morris, "Feedback Control of Dynamic Bipedal Robot Locomotion," CRC Press, Boca Raton, June 2007.

[4] A. D. Ames, R. Vasudevan, and R. Bajcsy, "Human-Data Based Cost of Bipedal Robotic Walking," In 14th Int. Conf. on Hybrid Systems: Computation and Control, pp. 153-162, Chicago, April 2011.

[5] R. W. Sinnet, M. J. Powell, R. P. Shah, and A. D. Ames, "A Human-Inspired Hybrid Control Approach to Bipedal Robotic Walking," In 18th IFAC World Congress, pp. 6904-6911, Milan, September 2011.

[6] R. W. Sinnet and A. D. Ames, "3D Bipedal Walking with Knees and Feet: A Hybrid Geometric Approach," In 48th IEEE Conf. on Decision and Control and 28th Chinese Control Conf., pp. 3208-3213, Shanghai, December 2009.

[7] A. D. Ames, "First Steps Toward Automatically Generating Bipedal Robotic Walking from Human Data," In 8th Int. Workshop on Robotic Motion and Control, RoMoCo'11, Gronów, June 2011.

[8] A. D. Ames, E. A. Cousineau, and M. J. Powell, "Dynamically Stable Bipedal Robotic Walking with NAO via Human-Inspired Hybrid Zero Dynamics," In Hybrid Systems: Computation and Control, Beijing, 2012.

[9] A. D. Ames, R. W. Sinnet, and E. D. B. Wendel, "Three-Dimensional Kneed Bipedal Walking: A Hybrid Geometric Approach," In R. Majumdar and P. Tabuada (Eds.), 12th ACM Int. Conf. on Hybrid Systems: Computation and Control, Lecture Notes in Computer Science – HSCC 2009, Vol.5469, pp. 16-30, San Francisco, Springer Verlag, April 2009.

[10] J. W. Grizzle, C. Chevallereau, A. D. Ames, and R. W. Sinnet, "3D bipedal robotic walking: models, feedback control, and open problems," In IFAC Symposium on Nonlinear Control Systems, Bologna, September 2010.

[11] B. Morris and J. W. Grizzle, "A Restricted Poincaré Map for Determining Exponentially Stable Periodic Orbits in Systems with Impulse Effects: Application to Bipedal Robots," In 44th IEEE Conf. on Decision and Control and European Control Conf., Sevilla, December 2005.

[12] R. W. Sinnet, M. J. Powell, S. Jiang, and A. D. Ames, "Compass Gait Revisited: A Human Data Perspective with Extensions to Three Dimensions," In 50th IEEE Conf. on Decision and Control and European Control Conf., Orlando, December 2011.

[13] R. M. Murray, Z. Li, and S. S. Sastry, "A Mathematical Introduction to Robotic Manipulation," CRC Press, Boca Raton, March 1994.

[14] Y. Hürmüzlü and D. B. Marghitu, "Rigid body collisions of planar kinematic chains with multiple contact points," Int. J. of Robotics Research, Vol.13, No.1, pp. 82-92, February 1994.

[15] J. E. Marsden and T. S. Ratiu, "Introduction to Mechanics and Symmetry," Vol.17 of Texts in Applied Mathematics, Springer, 1999.

[16] A. D. Ames, "A Categorical Theory of Hybrid Systems," Ph.D. thesis, University of California, Berkeley, 2006.

[17] A. D. Ames and R. D. Gregg, "Stably Extending Two-Dimensional Bipedal Walking to Three Dimensions," In American Control Conf., pp. 2848-2854, July 2007.

[18] S. H. Collins and A. Ruina, "A Bipedal Walking Robot with Efficient and Human-Like Gait," In IEEE Int. Conf. Robotics and Automation, pp. 1983-1988, Barcelona, April 2005.

3. http://youtu.be/hlnK5L9k1GU

Name:
Ryan W. Sinnet

Affiliation:
Graduate Student, Department of Mechanical Engineering, Texas A&M University

Address:
200 MEOB, 3123 TAMU, College Station, Texas 77843-3123, USA

Brief Biographical History:

2007 Received B.S. in Electrical Engineering from Caltech
2011 Received M.S. in Mechanical Engineering from Texas A&M University
2011- Pursuing Ph.D. as a Graduate Research Fellow of the National Science Foundation, Texas A&M University

Main Works:

• "A human-inspired hybrid control approach to bipedal robotic walking," in 18th IFAC World Congress, Milan, Sep. 2011.
• "3D bipedal walking with knees and feet: A hybrid geometric approach," in 48th IEEE Conf. on Decision and Control, Shanghai, Dec. 2009.

Membership in Academic Societies:

• American Society of Mechanical Engineers (ASME)
• The Institute of Electrical and Electronics Engineers (IEEE)
• American Mathematical Society (AMS)

Name:
Aaron D. Ames

Affiliation:
Assistant Professor, Department of Mechanical Engineering, Texas A&M University

Address:
200 MEOB, 3123 TAMU, College Station, Texas 77843-3123, USA

Brief Biographical History:

2001 Received B.S. in Mechanical Engineering and B.A. in Mathematics from the University of St. Thomas
2006 Received M.A. in Mathematics and Ph.D. in Electrical Engineering and Computer Sciences from U.C. Berkeley
2006-2008 Postdoctoral Scholar, the Control and Dynamical System Department, Caltech

Main Works:

• "First steps toward automatically generating bipedal robotic walking from human data," in Robotic Motion and Control (Lecture Notes in Control and Information Sciences), Vol.422, pp. 89-116, 2012.
• "Stably extending two-dimensional bipedal walking to three dimensions," in American Control Conf., 2007.

Membership in Academic Societies:

• The Institute of Electrical and Electronics Engineers (IEEE)